Retrieving broadband ultrashort THz wave packets through lossy channels

A. D. Koulouklidis,[1,2] V. Yu. Fedorov,[1,3,4] and S. Tzortzakis[1,2,4]

[1] *Institute of Electronic Structure and Laser (IESL), Foundation for Research and Technology - Hellas (FORTH), P.O. Box 1527, GR-71110 Heraklion, Greece*

[2] *Materials Science and Technology Department, University of Crete, 71003, Heraklion, Greece*

[3] *P. N. Lebedev Physical Institute of the Russian Academy of Sciences, 53 Leninskiy Prospekt, 119991, Moscow, Russia*

[4] *Science Program, Texas A&M University at Qatar, P.O. Box 23874 Doha, Qatar*

(Dated: November 4, 2015)

Most transmission and detection channels fail to faithfully support broadband wave packets because of physical limitations, like chromatic dispersion and absorption. We explore the case of lossy detection of ultrashort THz pulses using the widespread electro-optic detection scheme. We demonstrate that one can fully recover the original THz pulse shape, duration and amplitude, using a simple experimental procedure and a reconstruction algorithm which encodes the physical properties of the detection system.

arXiv:1511.00872v1 [physics.optics] 3 Nov 2015

INTRODUCTION

Nowadays electro-magnetic fields in the THz frequency range are of interest for a wide range of applications, including spectroscopy, nondestructive testing, tomographic imaging, and many others [1–5]. Modern THz sources are able to generate THz radiation with intensities high enough to observe nonlinear effects [6–8]. To date there are two major techniques for the generation of intense THz pulses on table-top setups: optical rectification in nonlinear crystals [9] and two-color filamentation (photoionization of gases by symmetry-broken laser fields) [10, 11]. Optical rectification allows one to generate THz pulses with very high energies (up to $900\,\mu$J) and spectral widths up to 5 THz [12]. In turn, THz pulses generated by two-color filamentation have less energy (up to $7\,\mu$J) but their spectrum is much broader, ranging from almost zero up to approximately 60 THz [13].

Although the generation of intense broadband THz radiation is a challenging task, its detection can be even more complicated. In the majority of THz applications we need a way to coherently detect a pulsed THz wave with a simultaneous measurement of its amplitude and phase. The most commonly used coherent detectors for THz radiation are photoconductive antennas [14, 15] and electro-optic crystals [16–18]. However, they have a limited detection bandwidth due to a finite carrier lifetime in antenna photocunductors and phonon resonances in electro-optic crystals. A typical THz pulse emitted during two-color filamentation has a spectrum which extends far beyond the detection limits of these two types of detectors. To date, the most broadband method for coherent detection of THz radiation is Air Biased Coherent Detection (ABCD) [19–21]. However the ABCD method is less sensitive than electro-optic detectors especially at low repetition rates, while its physical limitations are not fully studied. As a consequence, the majority of laboratories still use the electro-optic crystals as the main tool for coherent detection of THz radiation.

Since electro-optic detectors can measure only a small part of the generated THz spectrum, the detected THz electric field is strongly distorted. As a result, during electro-optic detection lots of information about the spectral content, shape and duration of the original THz pulse is lost. Although it may seem that this information is lost irrevocably, in this work we show how using a small number of realistic assumptions together with a simple experimental procedure one can retrieve the full information about the original THz wave packet and restore its parameters. Our reconstruction method is based on the nonlinear curve fitting of a recorded electro-optic signal. However, in contrast to the standard nonlinear curve fitting where the fitting function is expressed in a closed-form, our fitting function implements a numerical simulation of electro-optic detection. This method is accompanied by an experimental procedure where we stretch the input laser pulse in order to increase the duration of the generated THz pulses up to the point where their spectrum becomes narrower than the detection bandwidth of the electro-optic crystal. At this point we restore parameters of the generated THz pulses and appropriately extrapolate them to the region of the original THz pulse duration. As a result, we are able to retrieve the shape, duration, and absolute amplitude of the original THz pulse using only the partial information provided by the electro-optic detection.

I. THE EFFECT OF A LIMITED BANDWIDTH

At first let us demonstrate how the limited bandwidth of a detector affects our perception of a THz pulse.

In our experiments we generate THz pulses using the two-color filamentation scheme. Our Ti:sapphire chirped-pulse amplification laser system generates 39 fs (FWHM) pulses, at 800 nm central wavelength and maximum energy 2.3 mJ. We focus the input laser pulse by a lens with 200 mm focal length, followed by a $50\,\mu$m thick β-barium borate (BBO) Type-I crystal cut at 29.9° angle, which generates the second harmonic. After the BBO crystal, at the focus of the lens, the two-color pulses create a plasma filament that emits THz radiation. In order to avoid the absorption in water vapor we place our setup

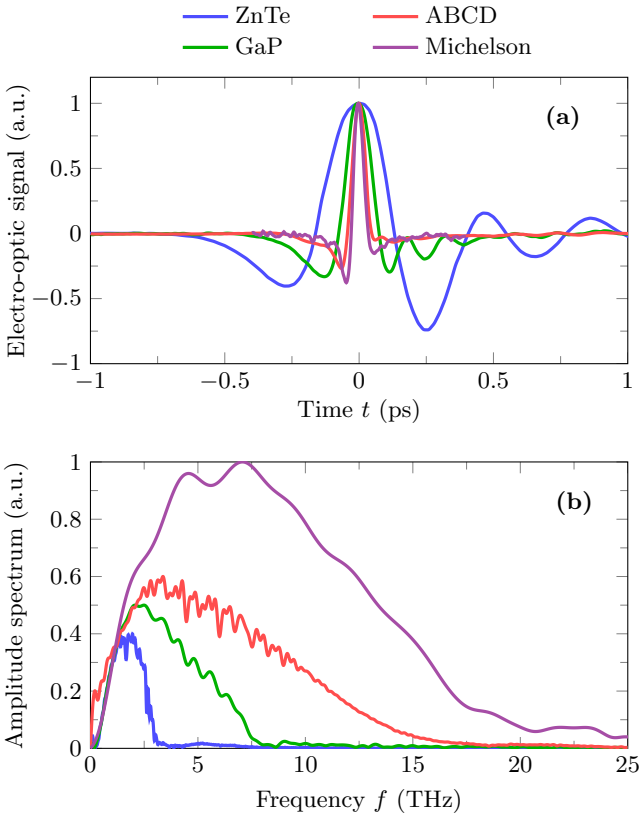

FIG. 1. Normalized THz electro-optic signals (a) and their amplitude spectra (b) for a THz pulse measured by different techniques, namely, by ZnTe and GaP electro-optic crystals, as well as by the ABCD method and Michelson interferometry (the spectra are normalized appropriately for clarity).

into a purge gas chamber filled with dry air. Using a pair of parabolic mirrors we gather the emitted THz radiation in the far field and send it to a THz detector. To detect the generated THz pulses we apply either electro-optic detection or ABCD measurements. For electro-optic detection we use 0.5 mm zinc telluride (ZnTe) and 100 μm gallium phosphide (GaP) crystals.

In addition to electro-optic and ABCD measurements we also conducted measurements of the generated THz pulses using Michelson interferometry as a reference method. We should stress that although originally Michelson interferometry is not a method of coherent detection (it cannot measure explicitly the phase of a THz pulse), it allows us though to detect the whole THz spectrum without limitations.

Figure 1 shows the signals and their amplitude spectra obtained by the different detection techniques. We see that the shortest spectrum is detected by the ZnTe crystal. It is followed by spectra measured by the GaP crystal and then by the ABCD measurement. The widest spectrum is registered by Michelson interferometry. The detection bandwidth of electro-optic crystals is mainly restricted by their transverse optical phonon resonances. In ZnTe crystals the first phonon resonance is located at 5.3 THz and in GaP at 11 THz [22]. In turn, the detection bandwidth of the ABCD method can be estimated as the inverse duration of the probe pulse (the main limiting parameter). In our experiments, the duration of the probe pulse is about 70 fs (the probe pulse is longer than the input pulse due to the dispersion in the guiding optics) which corresponds to a detection bandwidth of about 14 THz.

In Fig. 1 we also see that the signals obtained by the different detection techniques have different durations and shapes. To be more quantitative, let us define the duration τ_s of the detected signal as the duration of its first oscillation, i.e., the time between the first minimum and the first maximum of the signal. Using this definition, we find that the durations τ_s of the signals in Fig. 1 are the following: 275 fs for the ZnTe crystal, 127 fs for the GaP crystal, and 66 fs for the ABCD method. In principle, the signal from the Michelson interferometer does not reproduce the electric field of the incoming THz pulse. However, the period of the Michelson interferogram corresponds to such an optical path difference that the temporal delay between the pulses in the two arms of the Michelson interferometer is equal to the period of the detected THz electric field. Therefore, taking into account our definition of τ_s, we can use the Michelson interferogram in order to estimate the duration of the generated THz pulses. In Fig. 1 we see that the signal obtained by the Michelson interferometer shows a duration τ_s of 44 fs, which we assume to be the closest estimate of the actual THz pulse duration.

Thus, even using the best of our electro-optic crystals we measure the THz pulse duration being almost three times larger than its actual value. In addition, the signal from the electro-optic detectors leads us to wrong conclusions about the shape of the original THz pulses. Figure 1 shows that both ZnTe and GaP crystals predict additional field oscillations that are absent on the signal measured by the more precise ABCD method and the Michelson interferometry [23]. Thus, the electro-optic detection, although it presents very high sensitivity, strongly affects our perception of the THz electric field deforming its original shape and misleading about its duration.

In the following sections we demonstrate how one can actually use lossy channels, like the electro-optic detection, yet still be able to fully recover the original broadband wave packet.

II. THE RECONSTRUCTION METHOD

In this section we introduce our reconstruction method whose aim is to restore broadband wave packets that were strongly distorted by a transmission or detection channel with losses. The method is based on the nonlinear curve fitting algorithm applied to experimentally recorded signals. In this algorithm we choose as initial condition a fitting function that, we believe, provides the best fit to

a series of experimental data points. The fitting function can depend nonlinearly on a number of parameters, which are defined by the nonlinear curve fitting algorithm through successive iterations, starting from some initial estimates. Usually, the fitting function is expressed in a closed-form, that is, using a finite number of constants, variables, and certain well-known functions (roots, exponents, trigonometric functions, etc.). However, the fitting function can be replaced by any functional relation that provides a one-to-one correspondence between a set of input data points and data points to be fitted. In our reconstruction method we choose a model that represents an input wave packet and depends on a number of fitting parameters that we want to find (for example, duration and/or amplitude of the wave packet). The appropriate model can be found through some prior knowledge about the process of the wave packet generation or through additional measurements that are able to measure the wave packet with minimal distortions. Additionally, we choose a model that encodes the physical properties of the lossy channel. This model can also include other fitting parameters like, for example, the distance of the wave packet propagation and/or the dispersion coefficient. We use all of the above fitting parameters as the arguments of the fitting function which takes the model wave packet and simulates its propagation through the lossy channel. The output signal, obtained as the result of the simulation, is then compared to the experimentally recorded signal. Using the iterative nonlinear curve fitting algorithm we find the values of the fitting parameters which provide the best match between the simulated and experimental signals. As a result, we are able to retrieve the parameters of the input wave packet, before it was distorted by the lossy channel, and the unknown properties of the lossy channel itself. In the rest of this section we consider a specific case of lossy detection of ultrashort THz pulses by the electro-optic detection scheme.

In order to choose a model for a THz pulse that enters the electro-optic detection system, let us turn to the results of the ABCD method and Michelson interferometry (see Fig. 1). The signals obtained by these two techniques show that the original THz pulse is a single cycle pulse, whose electric field $E(t)$ can be modeled with the following function:

$$E(t) = E_0 \frac{t}{t_0} \exp\left(-\frac{t^2}{t_0^2}\right), \qquad (1)$$

where E_0 is the peak amplitude. The same expression for $E(t)$ is also predicted by the photocurrent model [24]. The details about the model and simulation of electro-optic detection can be found in the Appendix. As the duration of $E(t)$ in equation (1) we use the value $\tau_0 = 2t_0/\sqrt{2}$, which is defined as the time between the first minimum and the first maximum of the field, similar to the above definition of τ_s.

In our reconstruction method we use two fitting parameters, namely, the duration τ_0 of the initial THz pulse and the length d of the electro-optic crystal. We consider d as an additional fitting parameter in order to compensate errors rising from inaccurate determination of the crystal's length and cut angle together with possible misalignment of the crystal relative to the optical axis. As the initial estimates for τ_0 and d we use the duration τ_s of the recorded electro-optic signal and the length of an electro-optic crystal provided by its manufacturer. At this stage of the reconstruction we do not take into account the absolute value of the amplitude E_0 and consider only normalized electro-optic signals.

In practice, the measured electro-optic signal is represented by a sequence of samples recorded in a finite time window. The sampling interval and the size of the time window usually differ from the spacing and size of a numerical grid used in the simulations. Therefore, before applying our reconstruction method, we prepare the recorded electro-optic signal. First, we use the linear interpolation and zero padding in order to transfer the experimental signal to a numerical grid. Then, we smooth the result by convolving it with a scaled Hanning window. We apply this preparation procedure to all electro-optic signals as the first stage of our reconstruction method.

In order to test our reconstruction method, let us apply it to the signal measured by a 100 μm GaP crystal. On Fig. 2 we plot the experimental electro-optic signal (middle column) and its amplitude spectrum (right column) together with their best fits obtained by our reconstruction method for different models of the initial pulse (left column). One can clearly see that the model from Eq. (1) (top raw) gives the closest agreement with the experimental findings. However, the duration τ_0 of the original THz pulse, restored by our reconstruction method for this model, is equal to 84 fs. This value is unreasonably large, since we have already seen that according to Michelson interferometry the actual duration of the original THz pulse should be around 44 fs. In order to clarify this inconsistency we would like to remind that during electro-optic detection we lose a lot of information about the high-frequency part of the THz pulse spectrum. Therefore, if we consider two very short THz pulses with different durations such that their spectra are much wider than the detection bandwidth, then their electro-optic signals will be indistinguishable, because short THz pulses with the electric field from equation (1) have very similar low frequency spectrum. In other words, there is no unique solution for our reconstruction method in case of very short THz pulses. In practice, the initial estimate for τ_0 is the duration τ_s of a recorded electro-optic signal, which is longer than the original THz pulse. The reconstruction method starts to search successively for shorter durations and stops at the first one which provides a good fit. Thus our reconstruction method finds the longest possible THz pulse whose electro-optic signal fits the recorded one.

Let us make an additional test in order to clarify the amount of error that our reconstruction method produces during the retrieval of the original THz pulse duration. For this purpose let us consider several THz pulses of dif-

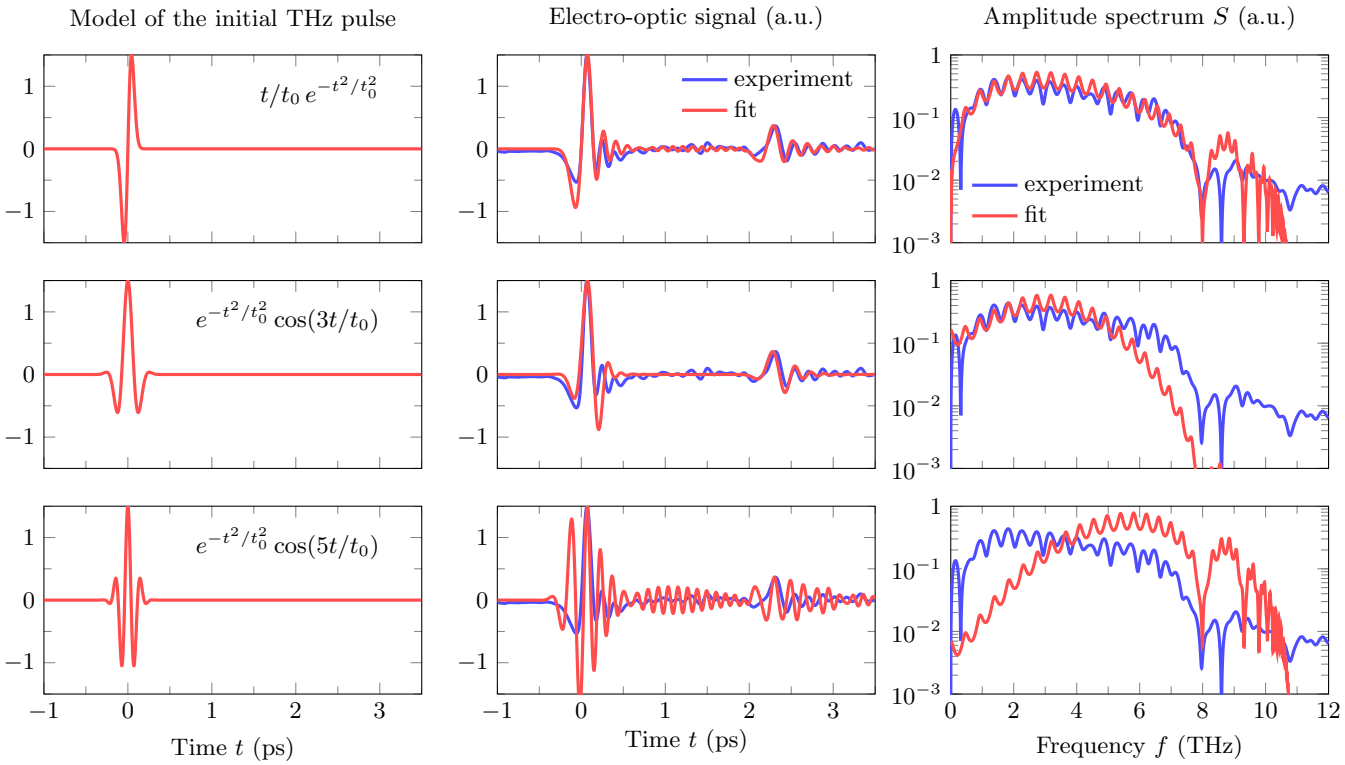

FIG. 2. The electro-optic signal measured by 100 μm Gap crystal (middle column) and its amplitude spectrum (right column) together with their best fits obtained by the reconstruction method for different models of the initial THz pulse (left column).

ferent durations τ_0 whose electric fields are calculated by equation (1). We simulate their electro-optic detection by the 100 μm GaP crystal and then apply our reconstruction method to the obtained results in order to retrieve the original value of τ_0. In order to reproduce the experimental conditions, in the simulated electro-optic signals we filtered out (using a supergauss filter) all frequencies that are higher than 8 THz. Despite the fact that the GaP phonon resonance is located at 11 THz, in the experiments we can not see any signal above 8 THz. One of the possible explanations is a low signal to noise ratio at these frequencies. Additionally, we use a 5 ps long segment from the numerical grid in order to reproduce a finite time window which we use in the experiment for sampling the experimental data.

Figure 3 shows the duration τ_{sim} of the simulated electro-optic signals and the corresponding duration τ_{res} restored by our reconstruction method as functions of the initial duration τ_0. The dashed line in Fig. 3 indicates an ideal case when the duration τ_{res} retrieved by the reconstruction method is equal to τ_0. Figure 3 shows that the duration τ_{sim} of the simulated electro-optic signal is always larger than the duration τ_0 of the original THz pulse. Although for longer THz pulses the difference between τ_{sim} and τ_0 decreases, due to the effects of THz pulse propagation inside the crystal, such as dispersion, the electro-optic detection still gives too high values. In Fig. 3 we see that for THz pulses whose duration τ_0 is

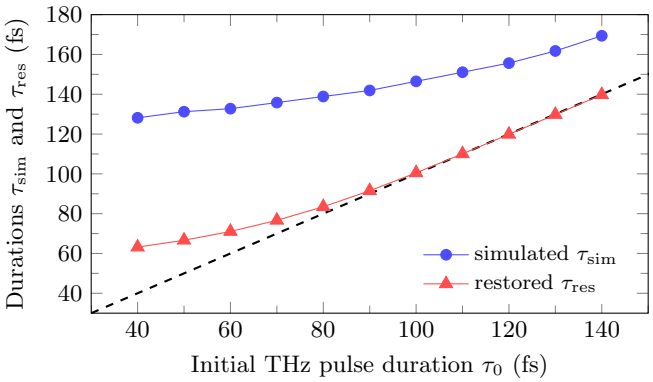

FIG. 3. The duration τ_{sim} of the simulated electro-optic signal and the corresponding duration τ_{res} obtained by the reconstruction method as functions of the initial THz pulse duration τ_0. Dashed line: see the text.

below than approximately 90 fs the restored duration τ_{res} is too high. In turn, for the THz pulses longer than 90 fs, the durations τ_{res} retrieved by our reconstruction method are exactly equal to the initial durations τ_0. The value of 90 fs is approximately the inverse of 11 THz which is the frequency of the GaP phonon resonance.

The results presented in Fig. 3 give us a hint about an additional procedure that will help us to retrieve the original duration of short THz pulses. Experimentally we can stretch the generated THz pulses up to the point

where the width of their spectra will be narrower than the detection bandwidth of the electro-optic crystal (according to Fig. 3 for 100 μm GaP crystal the appropriate durations must exceed 90 fs). For such long THz pulses we can apply our reconstruction method in order to exactly retrieve their original durations. Then we could use these findings and extrapolate them into the region of shorter THz pulses, given that there is a known correlation between the widths of the laser and the generated THz pulses. In the next section we show that such a correlation indeed exists.

III. THE CORRELATION BETWEEN THE LASER AND THZ PULSE DURATIONS

In this section we find the law according to which the duration of the generated THz pulse depends on the duration of the input laser pulse. In order to find this law we use the well accepted photocurrent model [24]. Since in the experiments the stretching of the laser pulse is usually achieved by changing the distance between the gratings of the laser compressor, the resulting pulse becomes chirped. Therefore, as the initial condition for the photocurrent model we use a chirped two-color pulse with the electric field $E(t)$ given by

$$E(t) = E_{\omega_0} A(t) e^{-i\omega_0 t} + E_{2\omega_0} A(t) e^{-i2\omega_0 t - i\pi/2}$$

and the envelope

$$A(t) = \frac{\sqrt{1+iC}}{\sqrt{1+C^2}} \exp\left[-(1+iC)\frac{t^2}{2t_f^2}\right],$$

where C is the chirp parameter, with $t_f = t_{f0}\sqrt{1+C^2}$ and t_{f0} being the durations of the stretched and transform-limited input laser pulse. As the central frequency ω_0 we choose the frequency that corresponds to 800 nm wavelength. Also we choose the amplitudes E_{ω_0} and $E_{2\omega_0}$ that correspond to the intensities I_{ω_0} and $I_{2\omega_0}$ such that $I_{2\omega_0} = 0.2 I_{\omega_0}$.

With the specified initial condition we calculate the photocurrent derivative $\partial J/\partial t$. As the generated THz pulse we consider a waveform that corresponds to the spectrum of $\partial J/\partial t$ at frequencies below 100 THz.

Since the initial two-color pulse is chirped, we need to take into account that its phase is strongly modulated. Therefore, in order to avoid errors in calculations of the amount of free electrons, we use a phase sensitive nonadiabatic ionization rate proposed by Yudin and Ivanov [25].

Figure 4 shows the dependence of the duration of the generated THz pulse as a function of the duration of the input laser pulse at different intensities I_{ω_0}. We see that independently of the initial intensity the duration of THz pulse depends linearly on the duration of the input laser pulse, and the slope of this linear dependence remains constant. This finding is of fundamental importance for the successful completion of our reconstruction process.

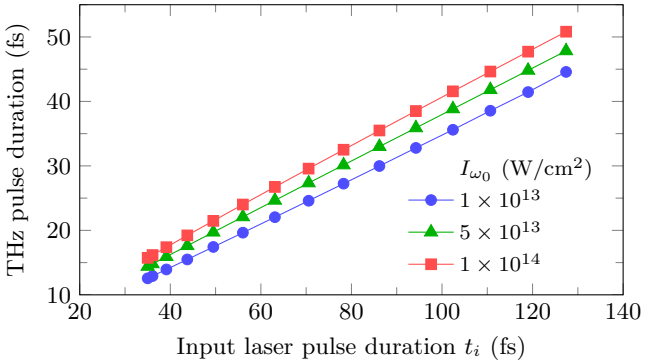

FIG. 4. The dependence of the THz pulse duration on the duration t_i of the input laser pulse, calculated using the photocurrent model.

Thus for our extrapolation procedure it is now justified to accept that the duration of the generated THz pulse depends linearly on the duration of the input laser pulse.

IV. RETRIEVED DURATION OF THE THZ PULSE

Now let us apply the combination of our reconstruction method and the extrapolation procedure to the experimental electro-optic signals. We conduct a series of experiments with the input laser pulses of different duration. For each experiment in the series we measure the FWHM duration τ_i of the input laser pulse and detect the corresponding generated THz pulses with a 100 μ GaP crystal. Then for each of the recorded electro-optic signals we apply our reconstruction method trying to retrieve the duration τ_0 of the original THz pulse.

Figure 5 shows the duration τ_s of the electro-optic signal measured by the GaP crystal and the corresponding duration τ_0 retrieved by our reconstruction method as a function of the input laser pulse duration τ_i. As a reference data, in this figure we also plot the durations τ_s measured by the ABCD method and the Michelson interferometer for the initial (shortest) laser pulse. If we compare the durations τ_s and τ_0 in Fig. 5 to the similar values in Fig. 3, we will find a familiar behavior. In Fig. 5 we see that for the input laser pulses whose duration τ_i exceeds 100 fs, the values of τ_0 retrieved by the reconstruction method depend linearly on τ_i. Since in the previous section we have shown that τ_i depends linearly on the duration of the generated THz pulses, we can use this data in order to linearly extrapolate these τ_0 values to the region of τ_i below 100 fs (stars in Fig. 5). As a result of the extrapolation, we find that the initial laser pulse with a duration $\tau_i = 39$ fs generates THz pulses with the duration $\tau_0 = 45$ fs. This value is almost identical to the duration of 44 fs measured by Michelson interferometry. Therefore, we can conclude that our reconstruction approach allows us to retrieve the actual duration of the generated THz pulses using only an electro-optic crystal

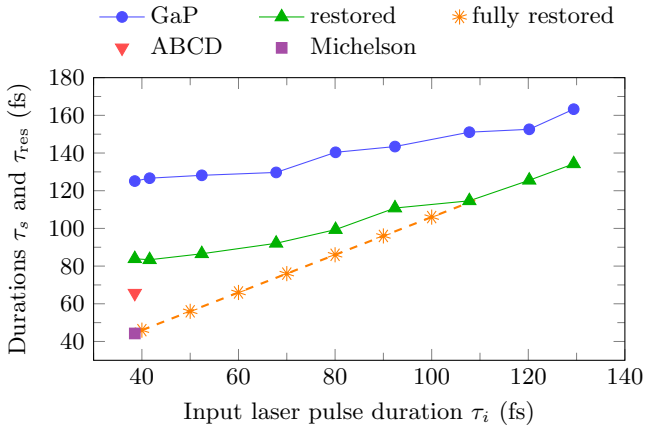

FIG. 5. The duration of the electro-optic signal τ_s and the corresponding duration τ_{res}, restored by the reconstruction method, as a function of the input laser pulse duration τ_i.

as the THz detector.

V. ABSOLUTE AMPLITUDE OF THE THZ PULSE

In the previous section we have shown how to retrieve the duration of the original THz pulse distorted by an electro-optic detector. One of the key assumptions of our reconstruction method is that the electric field of the original THz pulse can be well described by equation (1). The validity of this assumption is proved, on the one hand, by the measurements performed by the ABCD method and Michelson interferometry (see Fig. 1), and on the other hand, by the very good agreement between the experimental data and the numerical simulations (see Fig. 2).

The shape of the field in equation (1) depends only on one parameter $t_0 = \sqrt{2}\tau_0/2$. Therefore, since we are able to retrieve the duration τ_0, we can retrieve the exact shape of the original THz pulse. If, additionally, we find the way to retrieve the absolute amplitude E_0, we will retrieve all the information about the original THz wave packet.

There are two standard methods to calculate the absolute amplitude E_0 of a THz electric field if one uses electro-optic detection. In order to apply the first method we need to measure the total energy of a THz pulse. Additionally, for the same pulse, we need to measure its spatial distribution and electro-optic signal, then normalize them and integrate. The desired amplitude E_0 can be found if we divide the total THz energy by the two calculated integrals [26].

The second method is based on a simplified version of the theory of electro-optic detection (see Appendix) where we neglect the dispersion inside the electro-optic crystal. As a result of this simplification, we find that the peak of an electro-optic signal corresponds to a relative phase shift Γ given by [22]

$$\Gamma = \frac{2\pi n_0^3 d}{\lambda_0} r_{41} E_0, \tag{2}$$

where r_{41} is calculated at some specific frequency. The resulting value of E_0 is then calculated by equation (A.1), using the readings from the balanced photodiodes of the electro-optic detection setup.

Both these methods have substantial disadvantages. In the first method we assume that the temporal distribution of the THz field is well represented by an electro-optic signal which, as we have already seen, is not true. Moreover, this method demands additional measurements of the spatial profile of the THz pulse. In turn, the second method does not take into account the dispersion inside an electro-optic crystal.

As an alternative to the existing methods, we can calculate the absolute amplitude of the THz electric field using our reconstruction method. The calculation stages are the following. First, using a normalized electro-optic signal we restore the duration τ_0 of the initial THz pulse, thereby obtaining its shape, that is, its normalized electric field. Then, we simulate the electro-optic signal for a THz pulse with the restored duration τ_0 and a unit amplitude, let say 1 kV/cm. As a result, for a given THz pulse with a given τ_0, we find the relation between the absolute amplitude E_0 (in physical units) and the peak value of the corresponding electro-optic signal. The final scaling can be done using equation (A.1) and the readings from the balanced photodiodes. Thus our result will be the closest one to the actual value of the absolute amplitude, since it does not depend on additional measurements of the pulse profile and takes into account the distortions introduced by the electro-optic detector including the dispersion of the electro-optic crystal.

Now, let us determine the absolute amplitude of the THz pulse whose duration we have retrieved in the previous section. Following the above procedure, we find that our THz pulse with duration $\tau_0 = 45$ fs has peak amplitude E_0 equal to 250 kV/cm. For comparison, the amplitude calculated using equation (2) is equal to 70 kV/cm, which is 3 times lower than the value obtained by our reconstruction method.

VI. CONCLUSIONS

In conclusion, we have shown that one can fully retrieve ultrashort broadband THz wave packets that were severely transformed from dispersive and bandwidth lossy detection channels, like the very popular electro-optic detection. For achieving this we introduced a nonlinear curve fitting process in which we encoded the electro-optic detection physics, while we have also found a way to recover the lost bandwidth information, performing simple experiments, fully supported by the photocurrent model of THz generation. Our results beyond the evident impact on THz science and technology can

open the way in suggesting similar solutions to other problems in physics, optics and engineering, where only partial information of wave packets and wave functions can be measured.

Appendix: Model and simulation of electro-optic detection

Here we give a brief theoretical description of electro-optic detection and provide an algorithm for its numerical simulation. The electro-optic sampling technique is based on measuring the birefringence induced by THz pulses inside a detection crystal. To detect this induced birefringence we use a probe laser pulse that changes its polarization during the propagation through the detection crystal. After the crystal we split the probe laser pulse into two components with mutually perpendicular polarizations and send them to a pair of photodiodes. Let us denote the voltage in each of the photodiodes as A_1 and A_2. A normalized difference of A_1 and A_2 is given by [27]

$$\frac{A_1 - A_2}{A_1 + A_2} = \sin\Gamma, \tag{A.1}$$

where Γ is a relative phase shift between two orthogonally polarized components of the probe laser pulse. We can write Γ as [22]

$$\Gamma(t) = \frac{2\pi n_0^3 d}{\lambda_0}\mathrm{Re}[F(t)], \tag{A.2}$$

where λ_0 is the wavelength of the probe pulse, n_0 is the refractive index of the detection crystal at λ_0, and d is the crystal thickness. For GaP crystal at $\lambda_0 = 800\,\mathrm{nm}$ we have $n_0 = 3.18$ [22]. Factor $\mathrm{Re}[F(t)]$ in equation (A.2) denotes the real part of function $F(t)$ which we define as

$$F(t) = \frac{1}{2\pi}\int\limits_{-\infty}^{\infty} H(\omega)\,\widetilde{E}(\omega)e^{-i\omega t}d\omega. \tag{A.3}$$

Here $\widetilde{E}(\omega)$ is the spectrum of the incoming THz pulse with the electric field $E(t)$, that is,

$$\widetilde{E}(\omega) = \int\limits_{-\infty}^{\infty} E(t)e^{i\omega t}dt \tag{A.4}$$

and $H(\omega)$ is an electro-optic response function, given by [22]

$$H(\omega) = r_{41}(\omega)\,G(\omega)\,T(\omega), \tag{A.5}$$

where $r_{41}(\omega)$, $G(\omega)$, and $T(\omega)$ are the frequency dependent electro-optic coefficient, geometric response function, and transmission coefficient of the detection crystal, respectively.

The transmission coefficient $T(\omega)$ reads as

$$T = \frac{t_1 t_2 e^{ikd}}{1 + r_1 r_2 e^{2ikd}}. \tag{A.6}$$

If we assume that the detection crystal is surrounded by dry air with a unit refractive index, then $t_1 = 2/(1+n)$, $t_2 = 2n/(n+1)$, and $r_1 = (1-n)/(1+n)$, $r_2 = (n-1)/(n+1)$, where n is the refractive index of the detection crystal at THz frequencies with $k = n\omega/c_0$ being the wave number of the THz pulse.

For the frequency dependent refractive index n we use the following model [22]:

$$n^2(\omega) = \varepsilon_{el} + \frac{S_0\omega_0^2}{\omega_0^2 - \omega^2 - i\Lambda_0\omega}. \tag{A.7}$$

For a GaP crystal we take $\varepsilon_{el} = 8.7$, $S_0 = 1.8$, $\omega_0/(2\pi) = 10.98\,\mathrm{THz}$, and $\Lambda_0/(2\pi) = 0.02\,\mathrm{THz}$ [22].

The geometric response function $G(\omega)$ takes into account the mismatch between the phase velocity of the THz pulse and group velocity v_g of the probe laser pulse inside the detection crystal [22]:

$$\begin{aligned} G(\omega) &= \frac{1}{d}\int\limits_0^d dz \int\limits_{-\infty}^{\infty} \delta(z/v_g - t)e^{i(kz-\omega t)}dt \\ &= \frac{1}{d}\frac{e^{i(k-\omega/v_g)d} - 1}{i(k - \omega/v_g)}. \end{aligned} \tag{A.8}$$

For a probe pulse at the wavelength $\lambda_0 = 800\,\mathrm{nm}$ propagating inside a GaP crystal we have $v_g = 0.28c_0$ [22].

The electro-optic coefficient r_{41} determines the sensitivity of a detection crystal at different frequencies. We use the following model for r_{41} [22]:

$$r_{41}(\omega) = d_E\left(1 + \frac{C\omega_0^2}{\omega_0^2 - \omega^2 - i\Lambda_0\omega}\right) \tag{A.9}$$

with the same parameters ω_0 and Λ_0 as in the model for $n(\omega)$. For GaP crystals we use $d_E = 1.13\times10^{-12}\,\mathrm{m/V}$ and $C = -0.47$. These values of d_E and C slightly differ from the ones proposed in [22]. We modified the original values in order to shift the frequency where the real part of r_{41} becomes zero. This correction gives a better fit for our experimental data.

Equations (A.1)–(A.9) allow us to simulate the process of electro-optic sampling for any given THz pulse. Let us assume that we know the electric field $E(t)$ of an initial THz pulse, then the algorithm of the numerical simulation is the following: (i) calculate the spectrum $\widetilde{E}(\omega)$ of $E(t)$ in accordance with equation (A.4); (ii) using equations (A.6)–(A.9), calculate the electro-optic coefficient $r_{41}(\omega)$, geometric response function $G(\omega)$, and transmission coefficient $T(\omega)$; (iii) calculate the electro-optic response function $H(\omega)$ by equation (A.5) and then function $F(t)$ by equation (A.3); (iv) using equation (A.2), calculate the phase shift $\Gamma(t)$. The sine of Γ, according

to equation (A.1), gives us an electro-optic signal which we can directly compare with the experimental data.

For a practical realization of the nonlinear curve fitting algorithm we use PYTHON programming language and specifically the CURVE_FIT function from SCIPY.OPTIMIZE library [28]. This function implements the Levenburg-Marquardt algorithm for nonlinear curve fitting.

ACKNOWLEDGMENTS

We gratefully acknowledge the assistance Mrs. Christiana Alexandridi on the Michelson interferometry data. This work was partially supported by the EU Laserlab Europe and the Aristeia project FTERA (grant no 2570), co-financed by the European Union and Greek National Funds.

[1] M. Tonouchi, Nat. Photon. **1**, 97 (2007).
[2] B. Ferguson and X.-C. Zhang, Nat. Mat. **1**, 26 (2002).
[3] M. Jewariya, E. Abraham, T. Kitaguchi, Y. Ohgi, M.-a. Minami, T. Araki, and T. Yasui, Optics Express **21**, 2423 (2013).
[4] M. Massaouti, C. Daskalaki, A. Gorodetsky, A. D. Koulouklidis, and S. Tzortzakis, Appl. Spectrosc. **67**, 1264 (2013).
[5] J. Zhao, W. Chu, L. Guo, Z. Wang, J. Yang, W. Liu, Y. Cheng, and Z. Xu, Scientific reports **4**, 3880 (2014).
[6] D. Turchinovich, J. M. Hvam, and M. C. Hoffmann, Phys. Rev. B **85**, 201304 (2012).
[7] M. Zalkovskij, A. C. Strikwerda, K. Iwaszczuk, A. Popescu, D. Savastru, R. Malureanu, A. V. Lavrinenko, and P. U. Jepsen, Appl. Phys. Lett. **103**, 221102 (2013).
[8] J. Hebling, M. C. Hoffmann, K.-L. Yeh, G. Tóth, and K. A. Nelson, in *Ultrafast Phenomena XVI* (2009) pp. 651–653.
[9] W. R. Huang, S.-W. Huang, E. Granados, K. Ravi, K.-H. Hong, L. E. Zapata, and F. X. Kärtner, J. Mod. Opt. **62**, 1 (2014).
[10] K. Y. Kim, A. J. Taylor, J. H. Glownia, and G. Rodriguez, Nat. Photon. **2**, 605 (2008).
[11] T. I. Oh, Y. S. You, N. Jhajj, E. W. Rosenthal, H. M. Milchberg, K. Y. Kim, T. I. Oh, Y. S. You, N. Jhajj, E. W. Rosenthal, H. M. Milchberg, and K. Y. Kim, Appl. Phys. Lett. **102**, 201113 (2013).
[12] C. Vicario, A. V. Ovchinnikov, S. I. Ashitkov, M. B. Agranat, V. E. Fortov, and C. P. Hauri, Opt. Lett. **39**, 6632 (2014).
[13] T. I. Oh, Y. S. You, N. Jhajj, E. W. Rosenthal, H. M. Milchberg, and K. Y. Kim, New Journal of Physics **15**, 75002 (2013).
[14] I. Brener, D. Dykaar, A. Frommer, L. N. Pfeiffer, J. Lopata, J. Wynn, K. West, and M. C. Nuss, Opt. Lett. **21**, 1924 (1996).
[15] Y. Cai, I. Brener, J. Lopata, J. Wynn, L. Pfeiffer, and J. Federici, Appl. Phys. Lett. **71**, 2076 (1997).
[16] Q. Wu and X.-C. Zhang, Appl. Phys. Lett. **67**, 3523 (1995).
[17] A. Nahata, D. H. Auston, T. F. Heinz, and C. Wu, Appl. Phys. Lett. **68**, 150 (1996).
[18] C. Kubler, R. Huber, and A. Leitenstorfer, Semiconductor Science and Technology **20**, S128 (2005).
[19] J. Dai, J. Liu, and X.-C. Zhang, IEEE Journal of Selected Topics in Quantum Electronics **17**, 183 (2011).
[20] X. Lu and X.-C. Zhang, Appl. Phys. Lett. **98**, 151111 (2011).
[21] Z. Lü, D. Zhang, C. Meng, L. Sun, Z. Zhou, Z. Zhao, and J. Yuan, Appl. Phys. Lett. **101**, 081119 (2012).
[22] S. Casalbuoni, H. Schlarb, B. Schmidt, P. Schmüser, B. Steffen, and A. Winter, Physical Review Special Topics - Accelerators and Beams **11**, 072802 (2008).
[23] H. J. Bakker, G. C. Cho, H. Kurz, Q. Wu, and X.-C. Zhang, Journal of the Optical Society of America B **15**, 1795 (1998).
[24] K.-Y. Kim, J. H. Glownia, A. J. Taylor, and G. Rodriguez, Optics Express **15**, 4577 (2007).
[25] G. L. Yudin and M. Y. Ivanov, Phys. Rev. A **64**, 013409 (2001).
[26] F. Blanchard, G. Sharma, X. Ropagnol, L. Razzari, R. Morandotti, and T. Ozaki, Optics Express **17**, 6044 (2009).
[27] M. Brunken, H. Genz, C. Hessler, H. Loos, A. Richter, P. Göttlicher, M. Hüning, H. Schlarb, S. Simrock, P. Schmüser, D. Suetterlin, M. Tonutti, and D. Türke, *Electro-Optic Sampling at the TESLA Test Accelerator: Experimental Setup and First Results*, Tech. Rep. (TESLA Technology Collaboration, 2003).
[28] "Reference guide for the CURVE_FIT function," Available at: `http://docs.scipy.org/doc/scipy-0.13.0/reference/generated/` (Accessed: 13 September 2015).